

Object Recognition by Using Multi-level Feature Point Extraction

Yang Cheng, Timeo Dubois

1 Abstract

In this paper, we present a novel approach for object recognition in real-time by employing multi-level feature analysis and demonstrate the practicality of adapting feature extraction into a Naive Bayesian classification framework that enables simple, efficient, and robust performance. We also show the proposed method scales well as the number of level-classes grows. To effectively understand the patches surrounding a keypoint, the trained classifier uses hundreds of simple binary features and models class posterior probabilities. In addition, the classification process is computationally cheap under the assumed independence between arbitrary sets of features. Even though for some particular scenarios, this assumption can be invalid. We demonstrate that the efficient classifier nevertheless performs remarkably well on image datasets with a large variation in the illumination environment and image capture perspectives. The experiment results show consistent accuracy can be achieved on many challenging dataset while offer interactive speed for large resolution images. The method demonstrates promising results that outperform the state-of-the-art methods on pattern recognition.

2 Introduction

In the literature, one common idea image feature extraction is to focus on finding strong features that is robust enough to deal with perspective changes, lighting variations, such as SIFT local patterns detection and combines the output of the classifiers. Plagemann et al.⁶ create a novel interest point detector for catching body components from depth images.

Identifying textured patches surrounding keypoints across images acquired under widely varying poses and lightning conditions is at the heart of many Computer Vision algorithms ¹. The resulting correspondences can be used to register different views of the same scene, extract 3D shape information, or track objects across video frames. Correspondences also play a major role in object category recognition and image retrieval applications ².

Because of its strength to fractional impediments and computational proficiency, acknowledgment of picture patches removed around distinguished key focuses is critical for some vision issues. Therefore, two fundamental classes of methodologies have been produced to accomplish power to point of view and lighting changes ³. The primary family depends on nearby descriptors intended to be invariant, or possibly hearty, to particular classes of distortions ⁴. An inferior depends on measurable learning procedures to figure a probabilistic model of the fix.

3 A Semi-naive Bayesian approach to patch recognition

Picture patches can be perceived on the premise of extremely straightforward and arbitrarily picked double tests that are gathered into choice trees and recursively parcel the space of all conceivable patches. By and by, no single tree is sufficiently discriminative when there are many classes. In any case, utilizing various trees and averaging their votes yields great outcomes in light of the fact that everyone parcels the component space in an unexpected way ⁵.

Formulation of Feature Combination Given the patch surrounding a key point detected in an image, our task is to assign it to the most likely class. Let $C_i, I= 1, H$ Be the set of classes and let $f_j, j= 1, N$ Be the set of binary features that will be calculated over the patch we are trying to classify. Formally, we are looking for

$$C_i = \underset{C}{\operatorname{argmax}} P(C = c_i | f_1, f_2, \dots, f_N)$$

Where C is a random variable that represents the class. Bayes's formula yields

$$P(C = c_i | f_1, f_2, \dots, f_N) = \frac{P(C = c_i) \prod_{j=1}^N P(f_j | C = c_i)}{P(f_1, f_2, \dots, f_N)}$$

[As the denominator is simply a scaling factor, it can be reduced to]

$$C_i = \underset{C}{\operatorname{argmax}} P(C = c_i | f_1, f_2, \dots, f_N)$$

$$f_j = \begin{cases} 1 & \text{if } I(d_{j,1}) < I(d_{j,2}) \\ 0 & \text{otherwise} \end{cases}$$

Where I represents the image patch ⁷. (As the features specified are pretty simple, so $N = 300$.)

So)

$$P(f_1, f_2, \dots, f_N | C = c_i) = \prod_{j=1}^N P(f_j | C = c_i)$$

4 Comparison With Randomized Trees

As shown in Figures 3 and 4, Ferns can be considered as simplified trees. To compare RTs and Ferns, we experimented with the three images of Figure 5.

Greeneries vary from trees in two vital regards: The probabilities are increased in a Naive-Bayesian manner as opposed to being arrived at the midpoint of and the various leveled structure is supplanted by a level one.

The preparation set is acquired by arbitrarily twisting pictures of Figure 5. To play out these

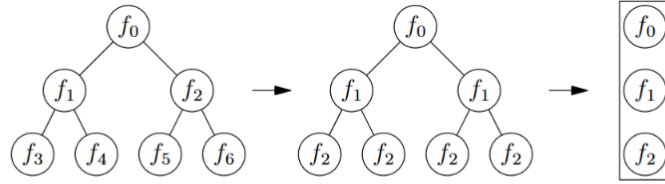


Fig. 3. Ferns vs Trees. A tree can be transformed into a Fern by performing the following steps. First, we constrain the tree to systematically perform the same test across any given hierarchy level, which results in the same feature being evaluated independently of the path taken to get to a particular node. Second, we do away with the hierarchical structure and simply store the feature values at each level. This means applying a sequence of tests to the patch, which is what Ferns do.

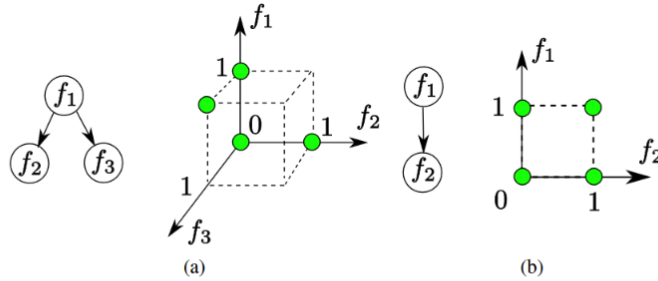


Fig. 4. The feature spaces of Trees and Ferns. Although the space of tree features seems much higher dimensional, it is not because only a subset of features can be evaluated. (a) For the simple tree on the left only the 4 combination of feature values denoted by green circles are possible. (b) The even simpler Fern on the left also yields 4 possible combinations of feature values but a much simpler structure. As shown below, this simplicity does not entail any performance loss.



Fig. 5. The recognition rate experiments are performed on three images that show different texture and structures. Image size is 640×480 pixels.

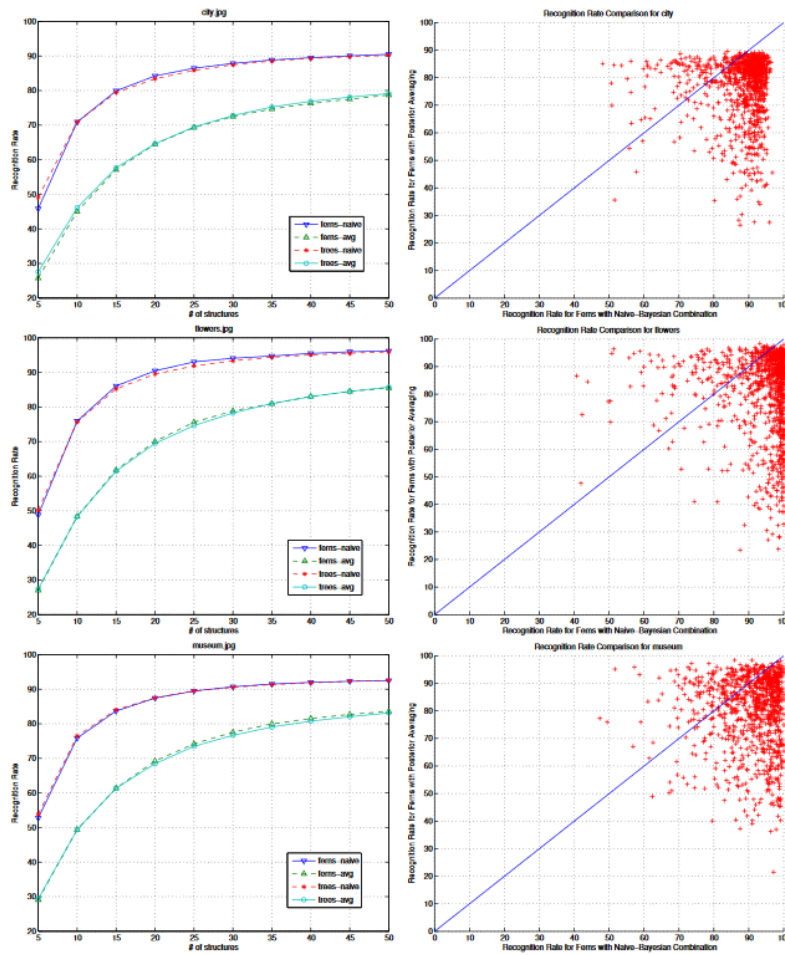
examinations, we speak to relative picture disfigurements as 22 networks of the shape.

$$R_0 R_{-\emptyset} \text{diag}(\lambda_1, \lambda_2) R_{\emptyset}$$

Where $\text{diag}(\lambda_1, \lambda_2)$ is a corner to corner 2×2 framework and R_{\emptyset} speaks to a revolution of point \emptyset . Both to prepare and to test our greeneries, we distorted the first pictures utilizing such misshapeness registered by arbitrarily picking λ_1 and λ_2 in the $[0: 2\pi]$ territory and θ_1 and θ_2 in the

[0.6: 1.5] territory. Fig. 6 delineates patches encompassing individual intrigue focuses first in the first pictures and after that in the distorted ones ⁷. We utilized 30 irregular relative distortions for each level of pivot to create 10800 pictures.

For the most part the test set is acquired by creating a different arrangement of 1000 pictures in a similar relative twisting extent and including clamor. In Figure 7, we plot the outcomes as an element of the quantity of trees or Ferns being utilized.



We first note that utilizing either level Fern or progressive tree structures does not influence

the acknowledgment rate, which was not out of the ordinary as the components are taken totally at irregular. Moreover as the scramble plots of Figure 7 appear, for the Naive-Bayesian blend the acknowledgment rate on individual twisted pictures never falls beneath a worthy rate.

5 Experiments

It is hard to play out a totally reasonable speed examination between our Ferns and SIFT for a few reasons ¹⁶. Filter reuses moderate information from the key guide extraction toward register canonic scale and introductions and the descriptors, while greeneries can depend on a minimal effort key-point extraction ⁸. Ferns vs SIFT to detect 3D objects So far we have considered that the key-focuses lie on a planar protest and assessed the heartiness of Ferns concerning viewpoint impacts. This rearranges preparing as a solitary view is adequate and the known 2D geometry can be utilized to figure ground truth correspondences. However most protests have really three dimensional appearance, which suggests that self-impediments and complex enlightenments impacts must be considered to effectively assess the execution of any key-point coordinating calculation ⁹.

Figure 11 shows such pictures traversing a 70? camera revolution go. We utilized this picture database to assess the execution of Ferns for an assortment of 3D items. We look at our outcomes against the SIFT identifier/descriptor match which has been found to perform extremely well on this database. The key-focuses and the descriptors are registered utilizing an indistinguishable programming from some time recently. We acquired the ground truth by utilizing simply geometric strategies, which is conceivable on the grounds that the cameras and the turn table are adjusted



Fig. 11. When detecting a 3D object viewpoint change is more challenging due to self-occlusions and non-trivial lighting effects. The images are taken from a database presented in [26] and cover a total range of 70° of camera rotation. They are cropped around the object, while we used the original images in the experiments. (a) *Horse* dataset. (b) *Vase* dataset. (c) *Desk* dataset. (d) *Dog* dataset.

¹⁰. The underlying correspondences are acquired by utilizing the trifocal geometry between the top/base cameras in the inside view and each other camera as outlined by Figure 12 ¹⁵. We then reproduce the 3D focuses for each such correspondence in the base/focus camera arrange casing and utilize these to frame the underlying tracks that traverse the $-35^\circ/+35^\circ$ rotation territory around a focal view. At last to build power against spurious tracks framed by anomalies, we take out

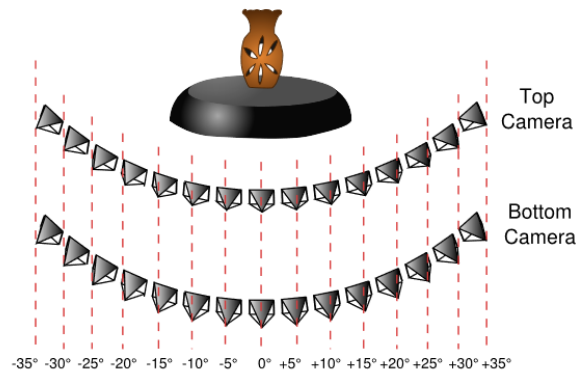


Fig. 12. Generating ground truth data for 3D object detection. Each test object contains two sequences of images taken by the *Top* and *Bottom* cameras while the object rotates on the turntable. The camera geometry has been calibrated using a checkerboard calibration pattern. We use 15 consecutive camera views for evaluation purposes, because it is easy to obtain high quality calibration for this range of rotation.

tracks covering less than 30percent of the perspectives and the rest of the tracks shape the ground

truth for the assessment ¹³, which is free of exceptions. Test ground truth information is portrayed by Figure 13, which demonstrates the mind boggling varieties in fix appearance incited by the 3D structure of the items ¹¹.

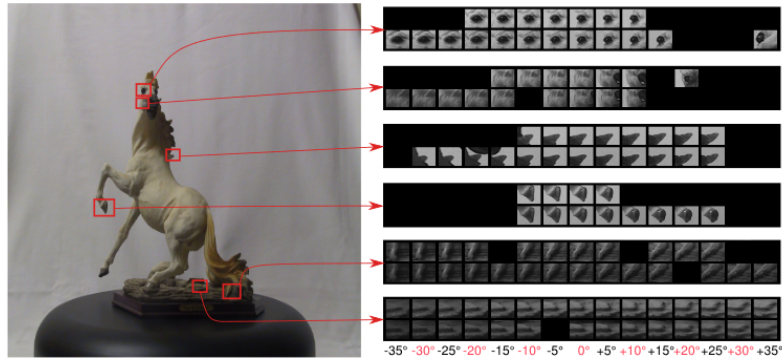


Fig. 13. Samples from the ground truth for the *Horse* dataset. The image on the left shows the center view. The six keypoint tracks on the right show the content variation for each patch as the camera center rotates around the turntable center. Each track contains two lines that correspond to the *Top* and *Bottom* cameras, respectively. Black areas denote frames for which the keypoint detector did not respond. The views produced by a rotation that is a multiple of 10° are used for training and are denoted by red labels. The others are used for testing.

6 Panorama and 3D Scene Annotation

With the current expansion of cell phones with huge handling power, there has been a surge of enthusiasm for building genuine applications that can consequently explain the photographs and give helpful data about spots of intrigue. We have tried Ferns on two such applications, comment of display scenes and parts of a verifiable working with 3D structure ¹⁴. Both applications run easily at casing rate utilizing a standard portable PC and an of the rack web camera. By applying standard improvements for implanted equipment, we have ported this execution onto a cell phone that keeps running at a couple outlines for every second.



Fig. 14. Recognition rates for 3D objects. Each pair of bars correspond to a test frame. The red bar on the left represents the rate for Ferns and the light green bar on the right the rate for Nearest Neighbor SIFT matching. The weighted averages over all frames also appear as dashed line for Ferns and solid line for NN-SIFT. The weights we use are the number of keypoints per frame.

7 Conclusion

We have introduced an intense strategy for picture fix acknowledgment that performs well even within the sight of extreme viewpoint twisting. A key part of our approach is the Naive-Bayesian blend of classifiers that obviously beats the averaging of probabilities we utilized as a part of prior work. We have demonstrated that such a credulous mix methodology is a beneficial option when the particular issue is not excessively delicate to the suggested autonomy suspicions.

8 References

1. Thomas Mrwald, Markus Liu, "Self-monitoring to improve robustness of 3D object tracking for robotics", Robotics and Biomimetics (ROBIO) 2011 IEEE International Conference on, pp.

2830-2837, 2013.

2. Jun-Sik Kim, Makoto Lee, Joo Xavier, Pedro Aguiar, Takeo Kanade, "6D pose estimation of textureless shiny objects using random ferns for bin-picking", Intelligent Robots and Systems (IROS) 2012 IEEE/RSJ International Conference on, pp. 3334-3341, 2012, ISSN 2153-0858.
3. J. Shen and J. Yang, "Automatic human animation for non-humanoid 3d characters," International Conference on Computer-Aided Design and Computer Graphics (CAD/Graphics), pp. 220-221, 2015.
4. Wei Xiong, Shue Ching Chia, Yue Chen, Weimin Huang, Jiayin Zhou, Yufeng Zhou, Wilson Gao, Kae Jack Tay, Henry Ho, "Prostate boundary segment extraction using cascaded shape regression and optimal surface detection", Engineering in Medicine and Biology Society (EMBC) 2014 36th Annual International Conference of the IEEE, pp. 2886-2889, 2010, ISSN 1557-170X.
5. Dominik Sibbing, Bastian Liu, Leif Kobbelt, "SIFT-Realistic Rendering", 3DTV-Conference 2013 International Conference on, pp. 56-63, 2015.
6. Shu Wang, Mei Xie, "Iris matching using ferns classifier", Wavelet Active Media Technology and Information Processing (ICWAMTIP) 2012 International Conference on, pp. 109-112, 2014.
7. Ronny Hensch, Xiaohong Zhao, "Machine-learning based detection of corresponding interest points in optical and SAR images", Geoscience and Remote Sensing Symposium (IGARSS) 2014 IEEE International, pp. 1492-1495, 2016, ISSN 2153-7003.

8. Shaoguo Zhang, Yiyi Wei, Chunhong Pan, "BB-Homography: Joint Binary Features and Bipartite Graph Matching for Homography Estimation", *Circuits and Systems for Video Technology IEEE Transactions on*, vol. 25, pp. 239-250, 2011, ISSN 1051-8215.
9. J. Shen and S. C. S. Cheung, "Layer Depth Denoising and Completion for Structured-Light RGB-D Cameras," *IEEE Conference on Computer Vision and Pattern Recognition*, pp. 1187-1194, 2013.
10. Hideaki Uchiyama, Jia Li, Eric Marchand, "Toward augmenting everything: Detecting and tracking geometrical features on planar objects", *Mixed and Augmented Reality (ISMAR) 2011 10th IEEE International Symposium on*, pp. 17-25, 2015.
11. J. Shen, P. C. Su, S. c. S. Cheung, J. Zhao, "Virtual mirror rendering with stationary rgb-d cameras and stored 3-d background," *IEEE Transactions on Image Processing*, vol. 22, no. 9, pp. 3433-3448, 2013.
12. Taiki Fuji, Toshio Moriya, "Furniture layout AR application using floor plans based on planar object tracking", *RO-MAN 2012 IEEE*, pp. 670-675, 2002, ISSN 1944-9445.
13. Yasue Mitsukura, Wei Xiong, Yue Wang, Shue Ching Chia, Wenyu Chen, Jia Du, Ying Gu, Victor Ter Shen Kow, "CHORD: Cascaded and a contrario method for hole crack detection", *Image Processing (ICIP) 2015 IEEE International Conference on*, pp. 3300-3304, 2011.
14. Victor Eruhimov, Y. Konishi, C. Beltran, V. Murino, A. Del Bue, "Fast 6D pose from a single RGB image using Cascaded Forests Templates", *Intelligent Robots and Systems (IROS) 2016 IEEE/RSJ International Conference on*, pp. 4062-4069, 2010, ISSN 2153-0866.

15. E. Muoz, Wim Meeussen, "Outlet detection and pose estimation for robot continuous operation", Intelligent Robots and Systems (IROS) 2011 IEEE/RSJ International Conference on, pp. 2941-2946, 2010, ISSN 2153-0858.

16. J. Shen and W. Tan, "Image-based indoor place-finder using image to plane matching," IEEE International Conference on Multimedia and Expo, pp. 1-6, 2013.